Theoretical analysis of channel drop tunneling processes

Shanhui Fan, Pierre R. Villeneuve, and J. D. Joannopoulos
Department of Physics, Massachusetts Institute of Technology, 77 Massachusetts Avenue, Cambridge, Massachusetts 02139

M. J. Khan, C. Manolatou, and H. A. Haus
Department of Electrical Engineering and Computer Science, Massachusetts Institute of Technology, 77 Massachusetts Avenue, Cambridge, Massachusetts 02139
(Received 30 November 1998)

We investigate general channel drop tunneling processes using both analytic theory and first-principles simulations. These tunneling processes occur when two one-dimensional continuums are brought into close proximity with a resonator system that supports localized states. Propagating states can be transferred between the continuums through the resonator system. We show that the transport properties are intricately related to the symmetries of the resonant states. Complete transfer can be achieved by manipulating the symmetries of the system, and by forcing an accidental degeneracy between states with different symmetries. In addition, the line shape of the transfer spectrum can be engineered by varying the number of localized states in the resonator system. The theoretical analysis is confirmed by first-principles simulations of transport properties in a two-dimensional photonic crystal. [S0163-1829(99)09419-9]

I. INTRODUCTION

Resonant tunneling processes play an important role in many optical and electronic devices. Channel drop tunneling processes, in particular, have captured recent interest, due to their applications for wavelength division multiplexing in optical communication systems,[1,2,3] and potentially as a spectroscopy tool for electrons.[4] The processes occur between two one-dimensional continuums of propagating states, side coupled through a resonator system that supports localized states. Examples of the continuums include dielectric waveguides[2] and electronic nanowires,[5,6] while the resonator system could be made of optical cavities or quantum dots. Optimal tunneling is achieved when a selected propagation signal (i.e., monoenergy electron, or single-frequency photon) is completely transferred from one continuum to the other, leaving all other signals unaffected.

In a recent letter,[3] we determined the characteristics of the resonator system required to achieve complete channel drop tunneling. The characteristics were discussed for an exemplary structure supporting two localized states, which generated a transfer function with a Lorentzian line shape. In this paper, we introduce a formalism to determine the transport properties of general systems with an arbitrary number of resonances. The transport properties are related to the Green's-function matrix of the localized states, which is obtained by analyzing the direct and indirect coupling mechanisms. We derive criteria for complete transfer, and present structures that are capable of generating higher order transfer line shapes, such as the maximum-flat functions. The results of the analytic theory are verified by performing computational simulations on the transport properties of electromagnetic waves in two-dimensional photonic crystal structures.

The paper is organized as follows: In Sec. II, we present a detailed discussion of the formalism, and we derive criteria for the complete transfer in general systems. In Sec. III, we apply the formalism to analyze photonic crystal structures, and compare the theoretical results with computer simulations.

II. THEORY

The schematic diagram of a general system is shown in Fig. 1. The system is composed of two continuums, labeled C and $\overline{C}$, side coupled through a resonator system. The coordinates along the continuums are labeled x and $\overline{x}$, respectively. The continuums support propagating states. States in C are labeled $|q\rangle$, while states in $\overline{C}$ are labeled $|\overline{q}\rangle$, where q and $\overline{q}$ are wave vectors. The resonator system supports localized states. Localized states are labeled $|c\rangle$, where c is an integer, taking a value between 1 and the total number of localized states. The transport properties of the system are determined by interactions between these states.

We describe the interaction by an effective Hamiltonian H. The Hamiltonian consists of the sum of two parts H_0 and V where

$$H_0=\sum_k \omega_k|k\rangle\langle k|+\sum_c \omega_c|c\rangle\langle c|, \tag{1}$$

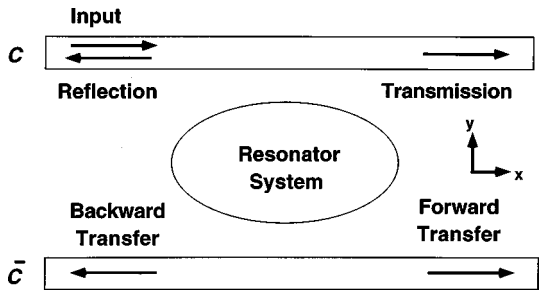

FIG. 1. Schematic diagram of two continuums coupled through a resonator system that supports localized states.

$$V=\sum_{c_1\neq c_2} V_{c_1,c_2}|c_1\rangle\langle c_2| + \sqrt{\frac{1}{L}}\cdot\sum_{k,c}\left[V_{c,k}|c\rangle\langle k|+V_{k,c}|k\rangle\langle c|\right]. \quad (2)$$

Here state $|k\rangle$ represents a state in either continuum, and ω_k is its frequency. The coefficient $V_{c,k}$ measures the coupling between a localized state $|c\rangle$ and a propagating state $|k\rangle$, while the coefficient V_{c_1,c_2} describes the strength of direct coupling between a pair of localized states $|c_1\rangle$ and $|c_2\rangle$. These coupling constants satisfy the conditions $V_{c,k}=V^*_{k,c}$ and $V_{c_1,c_2}=V^*_{c_2,c_1}$ due to the hermiticity of the Hamiltonian matrix. The $\sqrt{1/L}$ factor in Eq. (2) arises from a box normalization of length L. Similar Hamiltonians have been used by Fano[7] and by Anderson[8] to describe the interaction between localized resonances and continuums in different contexts.

A. Symmetry properties

The symmetry properties of the system impose certain constraints on the coupling constants. These constraints, as we will show in later sections, are of crucial importance to achieve complete transfer characteristics. Since the one-dimensional continuums define a propagation direction, the symmetry group in most cases consist only of mirror operators. With the existence of mirror symmetries, the coupling constants are no longer independent variables, but rather they are related to each other through symmetry operations. In addition, the continuums by themselves possess translational symmetry. Translational operators, while not being a symmetry operator of the entire structure, can nevertheless introduce interesting phase relations. We explore below the consequences of these symmetry operations.

1. Mirror operators

In general, there exist two types of mirror symmetries. Operator Π_x, which is perpendicular to the continuums, leaves each of the continuums invariant. Operator Π_y, which is parallel to the continuums, maps one continuum onto the other. We study the case where the Hamiltonian is invariant with respect to both operators, i.e.,

$$[\Pi_x,H]=0 \quad (3)$$

and

$$[\Pi_y,H]=0. \quad (4)$$

The propagating states in the continuums transform according to the following relations

$$\Pi_x|k\rangle=|-k\rangle, \quad (5)$$

$$\Pi_y|k\rangle=|\overline{k}\rangle. \quad (6)$$

Here, $|\overline{k}\rangle$ is defined as the propagating state with the same wave-vector value as the state $|k\rangle$, yet residing in a different continuum.

The localized states associated with the resonator system can be either even or odd with respect to the two mirror operators. For a state $|c\rangle$ that is even (odd) with respect to the operator Π_x, i.e.,

$$\Pi_x|c\rangle=+(-)|c\rangle, \quad (7)$$

the coupling constant must satisfy the following condition

$$V_{c,k}=+(-)V_{c,-k}, \quad (8)$$

as easily derived from Eq. (3). Similarly, For a state $|c\rangle$ that is even (odd) with respect to the Π_y operator, i.e.,

$$\Pi_y|c\rangle=+(-)|c\rangle \quad (9)$$

it follows from Eq. (4) that the coupling constant must satisfy the condition

$$V_{c,k}=+(-)V_{c,\overline{k}}. \quad (10)$$

2. Translational operators

To study the symmetry properties of the Hamiltonian H under translational transformations, we start by discussing the translational properties of the states associated with each individual component of the system, viewed as isolated entities. Since the continuums are translationally invariant, the propagating state $|k\rangle$ satisfies the Bloch theorem, i.e.,

$$T(a)|k\rangle=e^{-ika}|k\rangle, \quad (11)$$

where $T(a)$ represents a translation operation along the continuums by a distance a. The resonator system, on the other hand, does not possess translational symmetry. A state $|c\rangle$ localized at $x=0$, for example, is transformed into a state $|\tilde{c}\rangle\equiv T(a)|c\rangle$ localized at $x=a$.

Under the translational operation $T(a)$, the Hamiltonian H, therefore, is transformed into a new Hamiltonian $\tilde{H}=T(a)HT(a)^{-1}=\tilde{H}_0+\tilde{V}$, where

$$\tilde{H}_0=\sum_k \omega(k)|k\rangle\langle k|+\sum_c \omega_c|\tilde{c}\rangle\langle\tilde{c}| \quad (12)$$

and

$$\tilde{V}=\sum_{c_1\neq c_2} V_{c_1,c_2}|\tilde{c}_1\rangle\langle\tilde{c}_2| + \sqrt{\frac{1}{L}}\cdot\sum_{k,c}\left[V_{c,k}e^{ika}|\tilde{c}\rangle\langle k|+V_{k,c}e^{-ika}|k\rangle\langle\tilde{c}|\right]. \quad (13)$$

The first term on the right-hand side of Eq. (12) describes the continuums, and remains unchanged, as expected. A localized state $|c\rangle$ is transformed into the state $|\tilde{c}\rangle$. In addition, the coupling constants $V_{c,k}$ acquire wave-vector-dependent phase factors. Such changes in the coupling constants are analogous to gauge transformations, since both Hamiltonians H and $\tilde{H}$ describe the same physical system.

B. Transport properties

We now proceed to study the transport properties. In a gedanken experiment, we excite a state $|k\rangle$ at $x=-\infty$. The state propagates in C and excites the localized states in the

resonator system, which in turn decays along several directions in the continuums. This scattering process can be described in the usual way by the Lippman-Schwinger equation,[9] which relates the scattered wave function $|\psi\rangle$ to the incoming wave $|k\rangle$

$$|\psi\rangle = |k\rangle + \frac{1}{\omega_k - H_0 + i\varepsilon} V|\psi\rangle \equiv T|k\rangle. \tag{14}$$

In Eq. (14), ω_k is the frequency of the incoming wave, and ε is an infinitesimally small number greater than zero. The number ε is introduced to enforce an outgoing wave-boundary condition for the scattered wave.

Equation (14) can be solved iteratively. As a result, the T matrix can be represented as a sum of an infinite series

$$T_{k'k} \equiv \langle k'|T|k\rangle = \sum_{m=0}^{\infty} \langle k'| \left(\frac{1}{\omega_k - H_0 + i\varepsilon} V \right)^m |k\rangle. \tag{15}$$

Since there is no direct coupling between the propagating states, we can rewrite the infinite sum as

$$T_{k'k} = \delta_{k'k} + \frac{1}{\omega_k - \omega_{k'} + i\varepsilon} \sum_{c_1, c_2} V_{k', c_2} \cdot G_{c_2, c_1}(\omega_k) \cdot V_{c_1, k} \tag{16}$$

where

$$G_{c_2, c_1}(\omega) = \sum_{m=0}^{\infty} \left\langle c_2 \left| \frac{1}{\omega - H_0 + i\varepsilon} \left(V \frac{1}{\omega - H_0 + i\varepsilon} \right)^m \right| c_1 \right\rangle = \left\langle c_2 \left| \frac{1}{\omega - H + i\varepsilon} \right| c_1 \right\rangle \tag{17}$$

is the Green's function for a pair of localized states $|c_1\rangle$ and $|c_2\rangle$.

Equation (16) incorporates the effects from two physical processes. The incident wave can directly propagate into the final state, as described by the first term containing the delta function. Alternatively, the incident wave can excite the resonances, which in turn decay into the final state, as described by the second term. The sum of these two processes give the T matrix.

With Eq. (16), the scattering problem is reduced to the evaluation of a single-particle Green's function. Using standard diagrammatic perturbation method, the Green's function is evaluated exactly as

$$G = (1 - G^0 \Sigma)^{-1} G^0 \tag{18}$$

where G, G^0, and Σ are matrices with dimensions equal to the number of localized states. G^0 is the ''unperturbed'' Green's function for the localized states, and it is given by

$$G^0_{c_1, c_2} \equiv \left\langle c_1 \left| \frac{1}{\omega - H_0 + i\varepsilon} \right| c_2 \right\rangle = \frac{1}{\omega - \omega_{c_1} + i\varepsilon} \delta_{c_1, c_2}, \tag{19}$$

while Σ is the ''self-energy'' matrix, and is evaluated as

$$\Sigma_{c_1, c_2} = V_{c_1, c_2} + \frac{1}{L} \sum_q V_{c_1, q} \frac{1}{\omega - \omega_q + i\varepsilon} V_{q, c_2}. \tag{20}$$

The summation in Eq. (20) is performed over all propagating states in both continuums.

The poles of the Green's function in the complex ω plane determine the real and imaginary parts of the eigenfrequencies. By rewriting Eq. (18) as

$$G^{-1}_{c_1, c_2} = (\omega - \omega_{c_1}) \delta_{c_1, c_2} - \Sigma_{c_1, c_2}, \tag{21}$$

we can see that the off-diagonal elements of the self-energy matrix are related to the interactions between the localized states. The first term on the right-hand side of Eq. (20) represents a direct coupling mechanism. The second term describes an indirect coupling mechanism that occurs via the continuums: energy in a localized state couples into the continuums, propagates in the continuums, and then couples back into another localized state.

The structure of the Green's-function matrix can be simplified when the Hamiltonian possesses certain symmetries. We note that the operator G^{-1} possesses the same symmetry as the Hamiltonian, as can be seen by rewriting Eq. (21) in an operator form

$$G^{-1}_{c_1, c_2} = \left\langle c_1 \left| \left(\omega - H_0 - V - W \frac{1}{\omega - H_{\text{continuums}} + i\varepsilon} W \right) \right| c_2 \right\rangle \equiv \langle c_1 | G^{-1} | c_2 \rangle, \tag{22}$$

where $H_{\text{continuums}} \equiv \Sigma_q \omega_q |q\rangle\langle q|$ is the Hamiltonian for the continuums, and the matrix element of the W operator $W_{c,q} \equiv V_{c,q} |c\rangle\langle q|$ describes the interaction between the continuums and the localized states. The localized states $|c_1\rangle$ and $|c_2\rangle$ may belong to different irreducible representations of the symmetry group, or may transform as different partner functions for the same irreducible representation. In both cases, the off-diagonal element between the pair of states $|c_1\rangle$ and $|c_2\rangle$ vanishes. For many structures, symmetrizing the localized states alone is sufficient to completely diagonalize the Green's-function matrices.

In general, the Green's-function matrix can always be diagonalized by appropriately choosing a basis of localized states. In this basis, the Green's function for a localized state $|c\rangle$ can be written as

$$G_{c,c}(\omega) = \frac{1}{\omega - \omega_c - \Sigma_{c,c}}. \tag{23}$$

The real part of $\Sigma_{c,c}$ represents a shift in resonant frequency with respect to the bare frequency ω_c. The imaginary part of $\Sigma_{c,c}$ corresponds to the width of the resonance, which is related to the power decay rate from the localized state into the continuums. The norm square of $G_{c,c}(\omega)$ possesses a Lorentzian line shape centered at a ''renormalized'' resonant frequency $\tilde{\omega}_c = \omega_c + \text{Re}\,\Sigma_{c,c}$ with a width of γ_c equal to $\text{Im}\,\Sigma_{c,c}$.

From Eq. (20), the width of the resonance is evaluated as

$$\gamma_c=\frac{\pi}{L}\sum_q |V_{c,q}|^2\cdot\delta(\tilde{\omega}_c-\omega)=\frac{|V_{c,q_c}|^2}{g_0}+\frac{|V_{c,\bar{q}_c}|^2}{g_0}, \tag{24}$$

where g_0 is the density of states of the propagating mode at frequency $\tilde{\omega}_c$, and is equal to the inverse of group velocity at that frequency. In deriving Eq. (24), we assume that state $|c\rangle$ couples to both continuums. Contributions from the two propagation directions within each continuum are also taken into account.

By diagonalizing the Green's-function matrix, the formula for the T matrix derived in Eq. (16) can be simplified to

$$T_{k'k}=\delta_{k'k}+\frac{1}{\omega_k-\omega_{k'}+i\varepsilon}\sum_c V_{k',c}G_{c,c}V_{c,k}. \tag{25}$$

Each localized state contributes to the T matrix as an independent scattering path. The scattering property is determined by the interference of the different amplitudes along all possible paths.

We now calculate the transmission, reflection, and transfer spectra, by evaluating the amplitudes of the scattered wave function Ψ at $x,\bar{x}=\pm\infty$. The transmitted amplitude is given by

$$\begin{aligned}\langle x=\infty|\psi\rangle&=\langle x=\infty|T|k\rangle=\sum_{k'}\langle x=\infty|k'\rangle\cdot\langle k'|T|k\rangle\\&=\lim_{x\to\infty}\frac{L}{2\pi}\int dk'\frac{1}{\sqrt{L}}e^{ik'x}\left[\delta_{k'k}+\frac{1}{(\omega_k-\omega_{k'}+i\varepsilon)\cdot L}\sum_c V_{k',c}G_{c,c}V_{c,k}\right]\\&=\sqrt{\frac{1}{L}}\left[1-i\sum_c\frac{V_{k,c}V_{c,k}}{g_0}\cdot\frac{1}{\omega_k-\tilde{\omega}_c+i\left(\frac{V_{k,c}V_{c,k}}{g_0}+\frac{V_{\bar{k},c}V_{c,\bar{k}}}{g_0}\right)}\right]e^{ikx}.\end{aligned} \tag{26}$$

Scattering amplitudes along the other directions can be obtained in a similar fashion. The reflected amplitude is given by

$$\langle x=-\infty|\psi\rangle=(-i)\sqrt{\frac{1}{L}}\left[\sum_c\frac{V_{-k,c}V_{c,k}}{g_0}\cdot\frac{1}{\omega_k-\tilde{\omega}_c+i\left(\frac{V_{k,c}V_{c,k}}{g_0}+\frac{V_{\bar{k},c}V_{c,\bar{k}}}{g_0}\right)}\right]e^{ikx}, \tag{27}$$

the forward transfer amplitude is given by

$$\langle\bar{x}=\infty|\psi\rangle=(-i)\sqrt{\frac{1}{L}}\left[\sum_c\frac{V_{\bar{k},c}V_{c,k}}{g_0}\cdot\frac{1}{\omega_k\tilde{\omega}_c+i\left(\frac{V_{k,c}V_{c,k}}{g_0}+\frac{V_{\bar{k},c}V_{c,\bar{k}}}{g_0}\right)}\right]e^{ik\bar{x}}, \tag{28}$$

and the backward transfer amplitude is given by

$$\langle\bar{x}=-\infty|\psi\rangle=(-i)\sqrt{\frac{1}{L}}\left[\sum_c\frac{V_{-\bar{k},c}V_{c,k}}{g_0}\cdot\frac{1}{\omega_k-\tilde{\omega}_c+i\left(\frac{V_{k,c}V_{c,k}}{g_0}+\frac{V_{\bar{k},c}V_{c,\bar{k}}}{g_0}\right)}\right]e^{i(-\bar{k})\bar{x}}. \tag{29}$$

C. Criteria for optimal channel drop transfer

We now examine Eqs. (26)–(29) in order to derive the criteria for optimal channel drop transfer. Optimal transfer occurs when a selected propagating state is completely transferred from one continuum to the other, while states at other frequencies remain unperturbed. Such transfer requires the cancellation of the reflection amplitude. From Eq. (27), the reflection amplitude originates entirely from the decay of the localized states. Hence, at least two states are needed for the decaying amplitude to cancel in the reflection direction. Below we consider the criterion in two-state systems, and then generalize the criterion to any number of states.

1. Two-state system

We begin by considering a structure that supports only two localized states, and possesses a mirror plane symmetry perpendicular to both continuums. We assume that these two states possess a different symmetry with respect to the mirror plane, one even labeled $|\text{even}\rangle$, one odd labeled $|\text{odd}\rangle$. Since the states possess a different symmetry, the Green's-function matrix is diagonal, and the conditions for using Eqs. (26)–(29) are satisfied. Moreover, from Eq. (8) we find $V_{e,k}=V_{e,-k}$ and $V_{o,k}=-V_{o,-k}$. Therefore, the states contribute to the reflection amplitude [Eq. (27)] with opposite signs.

Since each state possesses a Lorentzian line shape, complete cancellation of reflection amplitude over the entire fre-

quency ranges occurs only when the two states are degenerate in frequency and linewidth. In general, because the symmetry of the structure is low and only one-dimensional irreducible representations are allowed, the localized states belong to different irreducible representations and an accidental degeneracy among the states must be forced (e.g., by modifying the structural parameter of the system in the appropriate manner).

When such degeneracy is indeed forced, the transmission amplitude vanishes. And from Eq. (28), complete transfer occurs at resonant frequency when $|V_{k,c}|^2=|V_{\bar{k},c}^{-}|^2$. This latter condition implies the two localized states must decay into the two continuums at an equal rate. Recalling Eq. (9), we see that such condition can be satisfied by imposing mirror plane symmetry parallel to the continuums.

The discussions above can be summarized as follows: in a two-state system, the structure must possess two mirror planes, one parallel, and one perpendicular to the continuums to achieve complete transfer. Furthermore, the two states must possess different symmetry with respect the perpendicular mirror plane. Also, an accidental degeneracy of both the real and imaginary parts of the frequencies must be forced between the two states. An intuitive discussion of this criterion can be found in Ref. 10. The criterion can also be derived in a phenomenological fashion using Haus's time-coupled-mode theory.[11]

The propagation directionality of the transferred state is related to the symmetry of the localized states with respect to the mirror plane parallel to the continuums, as easily verified by inserting Eqs. (8) and (10) into Eqs. (28) and (29). When both states are even, the transfer occurs in the forward direction, and the backward transfer amplitude vanishes. On the other hand, when the state $|\text{even}\rangle$ has odd symmetry and the state $|\text{odd}\rangle$ has even symmetry with respect to the parallel mirror plane, complete transfer occurs in the backward direction. In both forward or backward cases, the intensity transfer function has a Lorentzian line shape, as seen from Eqs. (28) and (29).

2. General systems with any number of states

In applications such as optical communications, it is sometimes desirable to have transfer functions with a line shape other than Lorentzian. Such line shape requires structures that support more than two localized states. Below, we generalize the previous discussions for the two-state system to systems with any number of states.

Similar to the two-state case, it is important for the general system to have two mirror planes, one parallel and one perpendicular, with respect to the continuums. Having the perpendicular mirror plane is necessary to achieve cancellation of reflection, while having the parallel mirror ensures that the eigenstates decay into both continuums at an equal rate.

Also, we note that the decay amplitudes from any two states interfere destructively in the reflection direction when they are of opposite symmetry with respect to the perpendicular mirror plane. It is possible, therefore, to design a structure with localized states arranged in pairs. The states in each pair possess opposite symmetry with respect to the perpendicular mirror plane. By forcing an accidental degeneracy between the states in each pair, reflection is completely eliminated.

In the general case, however, symmetry and degeneracy alone are not sufficient to guarantee complete transfer. As we will see below, the complex frequency of each pair must be adjusted appropriately in order to achieve 100% transfer efficiency.

As a specific example, we apply the generalized discussion above to a structure that is capable of achieving a maximum-flat line shape in intensity transfer. An example of a maximum-flat function is given by

$$T(\omega)=\frac{\gamma^4}{(\omega-\omega_0)^4+\gamma^4}. \tag{30}$$

Such a line shape is of great interest for optical communication applications, due to its desired ''flat-top'' and ''sharp-sidewall'' characteristics.[12]

Since each pair of degenerate states contributes a first-order pole to the amplitude response function, it is obvious that at least two pairs are needed to generate a transfer function such as the one described in Eq. (30). We consider a structure with four localized states. Among the different symmetry properties that these states might possess, we consider the case where each state possesses different symmetry properties with respect to two mirror planes. This case is particularly simple, as the Green's-function matrix is automatically diagonalized. Each state, therefore, is an eigenstate that possesses a Lorentzian line shape, and Eqs. (26)–(29) can be directly applied to calculate transport properties.

We label the states according to their symmetry properties. The state $|\text{even-odd}\rangle$, for example, is even with respect to the mirror plane perpendicular to the continuums, and odd with respect to the mirror plane parallel to the continuums. Since there are four states, we recognize two pairing scenarios: (a) scenario 1,

$$\omega_{\text{even-even}}=\omega_{\text{odd-even}}\equiv\omega_1, \tag{31}$$

$$\omega_{\text{even-odd}}=\omega_{\text{odd-odd}}\equiv\omega_2, \tag{32}$$

$$\gamma_{\text{even-even}}=\gamma_{\text{odd-even}}\equiv\gamma_1, \tag{33}$$

$$\gamma_{\text{even-odd}}=\gamma_{\text{odd-odd}}\equiv\gamma_2; \tag{34}$$

and (b) scenario 2,

$$\omega_{\text{even-even}}=\omega_{\text{odd-odd}}\equiv\omega_1, \tag{35}$$

$$\omega_{\text{even-odd}}=\omega_{\text{odd-even}}\equiv\omega_2, \tag{36}$$

$$\gamma_{\text{even-even}}=\gamma_{\text{odd-odd}}\equiv\gamma_1, \tag{37}$$

$$\gamma_{\text{even-odd}}=\gamma_{\text{odd-even}}\equiv\gamma_2. \tag{38}$$

In both scenarios, it follows from Eqs. (26)–(29) that a maximum-flat transfer function can be achieved by imposing the following conditions

$$\gamma_1 = \gamma_2, \tag{39}$$

$$\omega_1 - \omega_2 = 2\gamma. \tag{40}$$

We also note that, in the first scenario the wave is transferred along the forward direction, while in the second scenario the wave is transferred along the backward direction.

In addition, it is important to point out that the transfer can in fact be entirely eliminated when all four states have the same frequency and the same width, i.e.,

$$\omega_{\text{even-even}} = \omega_{\text{odd-even}} = \omega_{\text{even-odd}} = \omega_{\text{odd-odd}}, \tag{41}$$

$$\gamma_{\text{even-even}} = \gamma_{\text{odd-even}} = \gamma_{\text{even-odd}} = \gamma_{\text{odd-odd}}. \tag{42}$$

Thus, if the system were designed to be tunable, this result could allow for switching on and off the channel drop process, as well as for switching between forward and backward transfers.

In the following section, we validate the results of the theoretical analysis by studying transport properties of electromagnetic waves in photonic crystals. Photonic crystals offer an ideal environment for studying these processes. With the existence of a band gap, one can create one-dimensional continuums and resonators with desired number of modes, while eliminating all other modes, including radiation modes.

III. CHANNEL DROP PROCESSES IN PHOTONIC CRYSTALS

We consider a photonic crystal made up of a square lattice of high-index dielectric rods with a dielectric constant of 11.56 and a radius of $0.20a$, where a is the lattice constant of the square array. The band structure of a perfect crystal and the defect modes have been studied extensively.[13,14] We summarize here only the relevant results. The crystal possesses a complete band gap for the TM-polarized states, which has its electric field parallel to the rods. A line defect can be introduced by removing a row of rods. This line defect supports a single-guide mode band inside the band gap. Localized states are introduced inside the photonic crystal by creating point defects. These point defects are formed by either increasing or decreasing the radius of a rod. By reducing the radius of a rod, the defect can be made to support a single degenerate state. Making the radius larger leads to a doubly degenerate state. These properties are exploited to construct channel drop structures in the photonic crystal.

We simulate the propagation of electromagnetic waves in the photonic crystal using a finite-difference time-domain program[15] with perfectly matched layer boundary condition.[16] At the entrance to the photonic crystal waveguide, a specially designed waveguide made up of a line defect in a distributed Bragg reflector (DBR) is used to connect to the photonic crystal waveguide, so that light can propagate out of the photonic crystal with minimum reflection. Light propagating in such DBR waveguides can then be effectively absorbed by the perfectly matched layers. A pulse excitation scheme is used to characterize transport properties over a wide frequency range in a single simulation run.

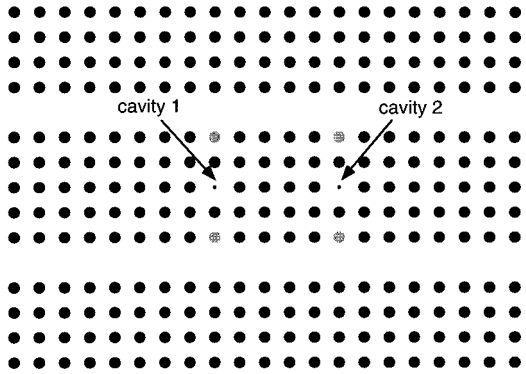

FIG. 2. Photonic crystal structure with two waveguides and two single-mode cavities used to achieve complete channel drop transfer. The black circles correspond to rods with a dielectric constant of 11.56, while the gray circles correspond to rods with a dielectric constant of 9.5. The two smaller rods define the cavities; they have a dielectric constant of 6.6, and a radius of $0.05a$, where a is the lattice constant.

A. Structure with two single-mode cavities

We first study a structure with two single-mode cavities as shown in Fig. 2. The structure possesses both the parallel and perpendicular mirror planes, as desired. It consists of two cavities, located at $d/2$ and $-d/2$ with respect to the origin located at the center of the figure. Each cavity is formed by reducing the radius of a rod, and supports a single localized state. The two states are labeled $|1\rangle$ and $|2\rangle$, respectively. The Hamiltonian H in Eqs. (1)–(2) can be written explicitly as

$$H_0 = \omega_0|1\rangle\langle 1| + \omega_0|2\rangle\langle 2| + \sum_{ko} \omega_k|k\rangle\langle k|, \tag{43}$$

$$V = \sqrt{\frac{1}{L}} \cdot \sum_k \{V_k e^{-ik(d/2)}|1\rangle\langle k| + V_k e^{ik(d/2)}|2\rangle\langle k| + V_{1,2}|1\rangle\langle 2| + \text{c.c.}\}. \tag{44}$$

Here, ω_0 is the unperturbed frequency of a single localized state in the absence of the waveguides. V_k represents the coupling constant between a single cavity and the waveguides when the cavity is placed at the origin. The phase factors $e^{ik(d/2)}$ and $e^{-ik(d/2)}$ are obtained by translational transformations, as derived in Eq. (13). The direct coupling constant $V_{1,2}$ becomes important when the two cavities are brought in close proximity with each other. Due to the mirror plane symmetry perpendicular to waveguides, it can be shown that $V_{1,2}$ must be real, and that $V_{1,2} = V_{2,1} \equiv V_x$.

Since the states $|1\rangle$ and $|2\rangle$ possess the same frequency when unperturbed, diagonalization of the Green's-function matrix is achieved by diagonalizing the self-energy matrix Σ. Using Eq. (20), we can write

$$\Sigma=\begin{bmatrix} \frac{1}{L}\sum_q |V_q|^2\frac{1}{\omega-\omega_q+i\varepsilon} & V_x+\frac{1}{L}\sum_q |V_q|^2\cdot e^{-iqd}\frac{1}{\omega-\omega_q+i\varepsilon} \\ V_x+\frac{1}{L}\sum_q |V_q|^2\cdot e^{iqd}\frac{1}{\omega-\omega_q+i\varepsilon} & \frac{1}{L}\sum_q |V_q|^2\frac{1}{\omega-\omega_q+i\varepsilon} \end{bmatrix}. \tag{45}$$

The summation in the matrix elements is evaluated using a contour integral method. As a result, Σ is calculated as

$$\Sigma=\begin{bmatrix} i\frac{2|V_{q_0}|^2}{g_0} & V_x-i\frac{2|V_{q_0}|^2}{g_0}e^{iq_0d} \\ V_x-i\frac{2|V_{q_0}|^2}{g_0}e^{iq_0d} & i\frac{2|V_{q_0}|^2}{g_0} \end{bmatrix}, \tag{46}$$

where q_0 and g_0 are the magnitudes of the wave vector and group velocity for the continuum states at the frequency ω_0, respectively. The factor 2 results from the presence of two continuums. The diagonal elements characterize the interaction of a single-cavity state with continuums on a single-cavity states. These elements are purely imaginary, indicating that the interactions introduce a finite lifetime, leaving the frequency unchanged. The off-diagonal elements incorporate the effects of both direct and indirect coupling mechanisms between the localized states, and affect both the frequency and the width of the states.

The matrix Σ is diagonalized by the symmetrization procedure

$$|\text{even}\rangle=\frac{1}{\sqrt{2}}(|1\rangle+|2\rangle), \tag{47}$$

$$|\text{odd}\rangle=\frac{1}{\sqrt{2}}(|1\rangle-|2\rangle), \tag{48}$$

where state $|\text{even}\rangle$ is even and state $|\text{odd}\rangle$ is odd with respect to the mirror plane perpendicular to the waveguides. The self-energy for the even and odd states is given by

$$\Sigma_{\text{even}}=V_x-\frac{2|V_{q_0}|^2}{g_0}\sin(q_0d)-i\cdot\frac{2|V_{q_0}|^2}{g_0}[1+\cos(q_0d)] \tag{49}$$

$$\Sigma_{\text{odd}}=-V_x+\frac{2|V_{q_0}|^2}{g_0}\sin(q_0d)-i\cdot\frac{2|V_{q_0}|^2}{g_0}[1-\cos(q_0d)]. \tag{50}$$

The resonant frequencies and widths of the resonant states are obtained from the self-energy expressions in Eqs. (49) and (50)

$$\tilde{\omega}_{\text{even}}=\omega_0+V_x-\frac{2|V_{q_0}|^2}{g_0}\sin(q_0d), \tag{51}$$

$$\tilde{\omega}_{\text{odd}}=\omega_0-V_x+\frac{2|V_{q_0}|^2}{g_0}\sin(q_0d), \tag{52}$$

$$\gamma_{\text{even}}=2\frac{|\cos(q_0d/2)V_{q_0}|^2}{g_0}, \tag{53}$$

$$\gamma_{\text{odd}}=2\frac{|\sin(q_0d/2)V_{q_0}|^2}{g_0}. \tag{54}$$

In obtaining these results, we assumed that both the wave vector and the group velocity of the propagating states associated with the line defects do not change appreciably when the frequency is varied within the width of the resonance peak. This is a good approximation since the width of the resonance is usually very narrow.

In order to achieve complete channel drop transfer from one continuum to the other, both the width and frequency of the resonant states must be made equal. The width of the resonances becomes equal when the following condition is satisfied

$$q_0d=n\pi+\pi/2, \tag{55}$$

which can be achieved by appropriately choosing the resonant frequency. The frequency splitting vanishes when

$$V_x-\frac{2|V_{q_0}|^2}{g_0}\sin(q_0d)=0. \tag{56}$$

The first term on the left-hand side of Eq. (56) represents the direct coupling mechanism, while the second term represents the indirect coupling. The frequency splitting is cancelled by a balance between these two mechanisms.

As a side note, when the condition $q_0d=(2n+1)\pi$ is satisfied, the width of the even state vanishes, while the width of the odd state reaches a maximum. For the even state, the two cavities oscillate in phase. Due to the spatial separation between the two cavities, at any given point in the waveguides, the decaying amplitudes are 180° phase out of phase and cancel each other. Similarly, when the condition $q_0d=2n\pi$ is satisfied, the width of the odd resonant state approaches zero while the width of the even resonant state approaches a maximum. This indicates a novel possibility of achieving a high-Q resonant state based on interference effects. We also note that the indirect part of the frequency splitting vanishes when the condition $q_0d=n\pi$ is satisfied.

The structure shown in Fig. 2 is designed to satisfy the degeneracy conditions given in Eqs. (55) and (56). In order

to satisfy Eq. (55), we choose the distance between the cavities to be $5a$, and the wave vector of the guided mode at the resonant frequency to be $0.25\,2\pi/a$. Examining Eq. (56), we note that the indirect part scales quadratically with the coupling constants, while the direct part scales linearly. Since the coupling constants decreases exponentially as the distance between the states increases, we choose the distance between the cavity and the waveguides to be $3a$, which is roughly equal to half the distance between the cavities. An exact degeneracy is enforced by changing the dielectric constant of four rods from 11.56 to 9.5. The position of these four rods is indicated by the light gray circles in Fig. 2.

For this structure, computer simulations indeed demonstrated complete channel drop tunneling, as published in a previous paper.[3] The simulated spectra agreed excellently with the theoretical results obtained using Eqs. (26)–(29).[3]

B. Structure with four single-mode cavities

Instead of using two localized states to achieve complete transfer, it may also be possible to use a resonator system with four states. The advantage of using more than two states is the possibility of creating a flat-top transfer function, as described in Sec. II C. Such a four-state structure is shown in Fig. 3. The resonator system is made up of four identical point defects in the photonic crystal. The structure possesses two mirror planes, as desired. Each defect supports a singly degenerate state. The state associated with the ith defect is labeled $|i\rangle$. Since the states possess the same frequency when uncoupled, it is sufficient to analyze the self-energy matrix Σ.

Using the method presented in Sec. III 1 for the two-state case, we calculate the Σ matrix as

$$\Sigma = \begin{bmatrix} i\dfrac{|V_{q_0}|^2}{g_0} & V_y & V_x - i\dfrac{|V_{q_0}|^2}{g_0}e^{iq_0d} & 0 \\ V_y & i\dfrac{|V_{q_0}|^2}{g_0} & 0 & V_x - i\dfrac{|V_{q_0}|^2}{g_0}e^{iq_0d} \\ V_x - i\dfrac{|V_{q_0}|^2}{g_0}e^{iq_0d} & 0 & i\dfrac{|V_{q_0}|^2}{g_0} & V_y \\ 0 & V_x - i\dfrac{|V_{q_0}|^2}{g_0}e^{iq_0d} & V_y & i\dfrac{V_{q_0}|^2}{g_0} \end{bmatrix}. \tag{57}$$

The above matrix could also have been obtained by simple inspection. Indirect coupling occurs only between states $|1\rangle$ and $|3\rangle$, and between states $|2\rangle$ and $|4\rangle$. Since each cavity interacts with only one continuum, the indirect coupling strength is half the value of that in the two cavity case. As for the direct coupling, we consider only nearest-neighbor interactions, as the amplitude of the defect states decays exponentially away from the defect. Since the structure has two mirror planes, there exist only two independent direct coupling constants, both of which are real; V_x is the direct coupling constant between states $|1\rangle$ and $|3\rangle$, and between states $|2\rangle$ and $|4\rangle$, and V_y is the direct coupling constant between states $|1\rangle$ and $|2\rangle$, and between states $|3\rangle$ and $|4\rangle$.

The Σ matrix is completely diagonalized by forming symmetrized states $|$even-even$\rangle$, $|$even-odd$\rangle$, $|$odd-even$\rangle$, and $|$odd-odd$\rangle$ as detailed earlier, each possessing a different symmetry with respect to the two mirror planes. The $|$even-odd$\rangle$ state, for example, is defined by

$$|\text{even-odd}\rangle = \tfrac{1}{2}(|1\rangle + |3\rangle - |2\rangle - |4\rangle), \tag{58}$$

and has even symmetry with respect to the perpendicular mirror plane, and odd symmetry with respect to the parallel mirror plane. These symmetrized states are the eigenstates of the system. Each state is associated with a single Lorentzian line shape, with a center frequency and a linewidth given by the following complex frequencies

$$\omega_{\text{even-even}} = \omega_0 + V_x + V_y + i\frac{|V_{q_0}|^2}{g_0}(1 - e^{iq_0d}), \tag{59}$$

$$\omega_{\text{odd-even}} = \omega_0 - V_x + V_y + i\frac{|V_{q_0}|^2}{g_0}(1 + e^{iq_0d}), \tag{60}$$

$$\omega_{\text{even-odd}} = \omega_0 + V_x - V_y + i\frac{|V_{q_0}|^2}{g_0}(1 - e^{-iq_0d}), \tag{61}$$

$$\omega_{\text{odd-odd}} = \omega_0 - V_x - V_y + i\frac{|V_{q_0}|^2}{g_0}(1 + e^{iq_0d}). \tag{62}$$

The real part of the complex frequency corresponds to the center frequency, while the imaginary part corresponds to the width of the Lorentzian.

To achieve a flat-top line shape, we configure the states in pairs, and create accidental degeneracies within the pairs of states $|$even-even$\rangle$ and $|$odd-even$\rangle$, and within the pair of states $|$even-odd$\rangle$ and $|$odd-odd$\rangle$, as discussed in Sec. II 3. To satisfy the constraints on the width as defined in Eqs. (33), (34), and (39), it is sufficient to have

$$q_0 d = n\pi + \pi/2, \tag{63}$$

which gives the same width γ for all four states, namely

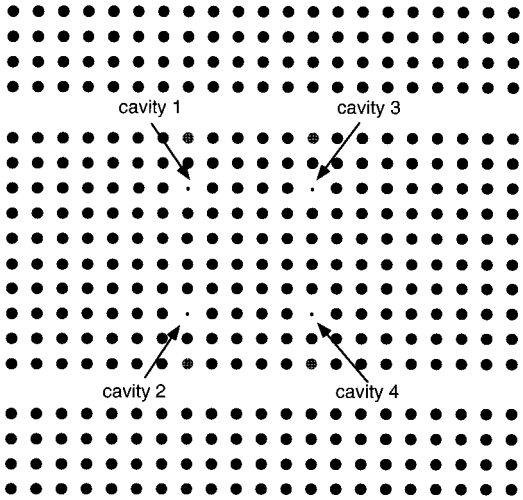

FIG. 3. Photonic crystal structure with two waveguides and four single-mode cavities. The black circles correspond to rods with a dielectric constant of 11.56, while the gray circles correspond to rods with a dielectric constant of 7.5. The four smaller rods define the cavities; they have a dielectric constant of 6.5, and a radius of $0.05a$, where a is the lattice constant.

$$\gamma = \frac{|V_{q_0}|^2}{g_0}. \tag{64}$$

The accidental frequency degeneracy constraints, as defined in Eqs. (31) and (32), are satisfied by imposing

$$V_x - \frac{|V_{q_0}|^2}{g_0} = 0. \tag{65}$$

When the accidental degeneracy is enforced, the maximum flat lineshape can be achieved by satisfying Eq. (40), which implies

$$V_y = \frac{|V_{q_0}|^2}{g_0}, \tag{66}$$

or equivalently,

$$V_x = V_y. \tag{67}$$

The structure shown in Fig. 3 is designed to satisfy all of the constraints described above. Equation (63) is satisfied by having the defects separated in the x direction by $5a$, and by appropriately setting the resonant frequency of the defect states such that $q_0 = 0.25(2\pi/a)$, where q_0 is the wave vector of the continuums at the resonant frequency. Equation (65) is satisfied by choosing the waveguide to be three lattice constants away from the cavity, and by changing the dielectric constant of four rods from 11.56 to 8.9 to achieve a cancellation between the direct and indirect coupling mechanisms. The four rods are indicated in light gray in Fig. 3. Equation (67) is satisfied by having the defects separated in the y direction by $5a$ as well.

We compute the filter response of the structure shown in Fig. 3 using a finite-difference time-domain scheme. A pulse is sent down one of the waveguides and excites the resonant states. These resonant states then decay exponentially into the waveguides. By Fourier transforming the decaying amplitudes, we can find the frequency spectrum of all the symmetric states, each with a Lorentzian line shape, as shown in Fig. 4. As required, the line shapes of the $|$even-even$\rangle$ and $|$odd-even$\rangle$ states overlap almost completely, as well as the line shapes of the $|$even-odd$\rangle$ and $|$odd-odd$\rangle$ states. The center frequency of the $|$even-even$\rangle$ state is separated from the center frequency of the $|$even-odd$\rangle$ state by twice the width of the resonant peak, as desired. Using these parameters, we compute the spectrum of the transmitted signal and that of the transferred signal using Eqs. (26)–(29). These spectra are shown as solid lines in Fig. 5 and are compared to those obtained by computational simulation (solid dots). Again, excellent agreement is obtained between theory and computer simulation. The transmission is close to 100% over the

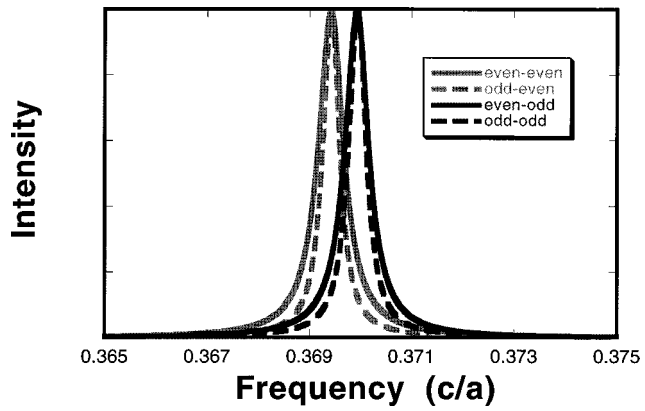

FIG. 4. Spectra of the four eigenmodes in the structure shown in Fig. 3.

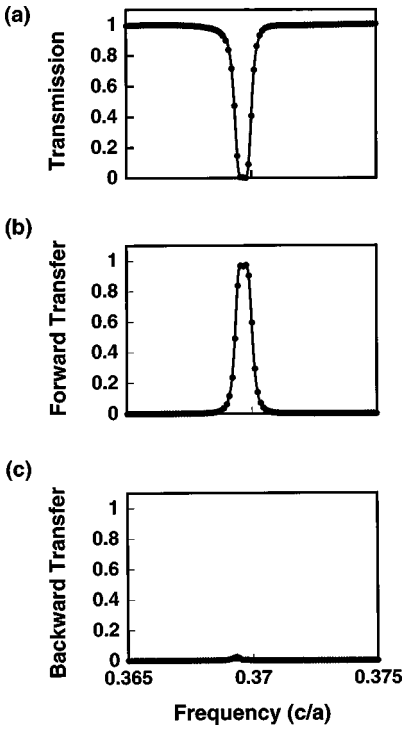

FIG. 5. Intensity spectra for the structure shown in Fig. 3: (a) transmission; (b) transfer in the forward direction; (c) transfer in the backward direction. The solid dots are obtained from computer simulations. The lines result from analytical theory.

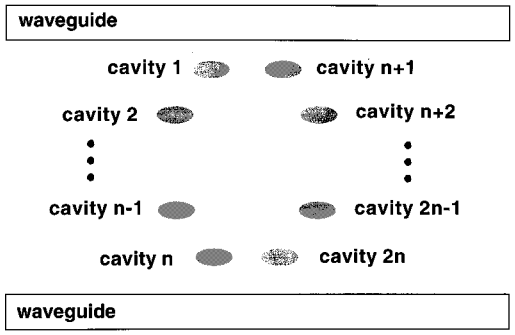

FIG. 6. Channel drop structure using $2n$ cavities. For clarity of presentation, only the position of the waveguides and cavities is indicated. The waveguides are represented by rectangles, and the cavities are represented by ellipses.

entire spectrum, except in the neighborhood of the center frequency where it drops to 0% [Fig. 5(a)]. The forward drop reaches a maximum close to 99% at the center frequency [Fig. 5(b)]. The backward drop shows almost complete absence of signal [Fig. 5(c)]. The transfer line shape does indeed show the maximum-flat characteristics, i.e., flattening of the top at the resonance peak and sharp falloff of the transfer amplitude away from the center frequency.

C. Structure with $2n$ cavities

Equations (61) and (63) provide a way to enforce degeneracies for a class of structures that consists of $2n$ identical single-mode cavities. A schematic is shown in Fig. 6. This structure is capable of generating a higher-order maximum flat line shape. The structure possesses the same two mirror planes as all the previous cases that we have discussed. The cavities can be separated into two groups. We label the cavities placed to the left of the perpendicular mirror plane with numbers 1 to n, forming the left group, and label the cavities on the right with numbers $n+1$ to $2n$, forming the right group. Cavity i is located at the image position of cavity $i+n$, with respect to the perpendicular mirror plane. An even state with respect to the perpendicular mirror plane can therefore be constructed by

$$|\text{even}\rangle = \sum_{i=1}^{n} c_i(|i\rangle + |i+n\rangle), \tag{68}$$

while its corresponding odd state is

$$|\text{odd}\rangle = \sum_{i=1}^{n} c_i(|i\rangle - |i+n\rangle). \tag{69}$$

Only cavities 1, n, $n+1$, and $2n$ interact with the continuums. Indirect coupling occurs between cavities 1 and $n+1$, and between cavities n and $2n$. The structure is configured such that direct coupling between the two groups occurs only between these two pairs. The direct coupling constant V_x must be real, as required by the mirror symmetries. With these information, the self energy matrix Σ assumes the following form

$$\Sigma = \begin{bmatrix} \Sigma_{\text{left}} & \Sigma_{\text{right-left}} \\ \Sigma_{\text{left-right}} & \Sigma_{\text{right}} \end{bmatrix}, \tag{70}$$

where each submatrix has the dimension $n \times n$. The diagonal submatrices Σ_{left} and Σ_{right} are equal. They are given by

$$\Sigma_{\text{left}} = \Sigma_{\text{right}} = \begin{bmatrix} i\dfrac{|V_{q_0}|^2}{g_0} & & & V_{\text{internal}} \\ & 0 & & \\ & & \cdots & \\ & & & 0 \\ V_{\text{internal}} & & & i\dfrac{|V_{q_0}|^2}{g_0} \end{bmatrix} \tag{71}$$

and describe the properties of each group of cavities. The off-diagonal submatrices, $\Sigma_{\text{left-right}}$ and $\Sigma_{\text{right-left}}$, are also identical, and describe the interactions between the two groups of cavities. They are given by

$$\Sigma_{\text{left-right}} = \Sigma_{\text{right-left}} = \begin{bmatrix} V_x - i\dfrac{|V_{q_0}|^2}{g_0} e^{iq_0 d} & & & 0 \\ & 0 & & \\ & & \cdots & \\ & & 0 & \\ 0 & & & V_x - i\dfrac{|V_{q_0}|^2}{g_0} e^{iq_0 d} \end{bmatrix}. \tag{72}$$

The Σ matrix can be block diagonalized by imposing the following condition

$$V_x - i\frac{|V_{q_0}|^2}{g_0} e^{iq_0 d} = 0. \tag{73}$$

Taking the real and imaginary parts of Eq. (73), we recover Eqs. (63) and (65). Under this condition, the two groups are completely decoupled. An accidental degeneracy between every even eigenstate and its corresponding odd eigenstate is thereby enforced. In the tunneling process, the reflection is completely absent. Of course, cancellation of reflection alone

is not a sufficient condition for complete transfer. The interaction within each group, as defined by V_{internal} in Eq. (71), still needs to be appropriately designed in order to achieve a desired line shape with 100% transfer efficiency.

IV. CONCLUSION

We have shown that the transport properties in a channel drop tunneling process can be described by the Green's function of the localized states. The Green's function can be determined by calculating the self-energy matrices. The tunneling processes occur when two one-dimensional continuums are brought in close proximity to a resonator system that supports multiple localized states. In such a system propagating states can be transferred between the continuums through the resonator system. We have shown that the transport properties are intricately related to the symmetries of the resonant states. By manipulating the symmetries and forcing an accidental degeneracy in the complex frequencies of the resonant states, complete transfer was achieved. In addition, the line shapes of the transfer spectra can be engineered by varying the number of localized states in the resonator system, and by properly designing the complex frequencies of these localized states. These results are quite general and are applicable to both photonic waveguide/microcavity systems as well as electroic quantum wire/quantum dot systems.

ACKNOWLEDGMENT

This work was supported in part by the MRSEC Program of the NSF under Award No. DMR-9400334.

[1] H. A. Haus and Y. Lai, J. Lightwave Technol. **10**, 57 (1992).
[2] B. E. Little, S. T. Chu, H. A. Haus, J. Foresi, and J.-P. Laine, J. Lightwave Technol. **15**, 998 (1997).
[3] S. Fan, P. R. Villeneuve, J. D. Joannopoulos, and H. A. Haus, Phys. Rev. Lett. **80**, 960 (1998).
[4] P. R. Villeneuve, S. Fan, and J. D. Joannopoulos (unpublished).
[5] C. C. Eugster and J. A. del Alamo, Phys. Rev. Lett. **67**, 3586 (1991).
[6] C. C. Eugster, J. A. del Alamo, M. J. Rooks, and M. R. Melloch, Appl. Phys. Lett. **64**, 3157 (1994).
[7] U. Fano, Phys. Rev. **124**, 1866 (1961).
[8] P. W. Anderson, Phys. Rev. **124**, 41 (1961).
[9] J. J. Sakurai, *Modern Quantum Mechanics* (Addison-Wesley, Redwood City, CA, 1985), p. 379.
[10] S. Fan, P. R. Villeneuve, J. D. Joannopoulos, and H. A. Haus, Opt. Express **3**, 4 (1998).
[11] C. Manolatou, M. J. Khan, S. Fan, P. R. Villeneuve, H. A. Haus, and J. D. Joannopoulos (unpublished).
[12] B. E. Little, S. T. Chu, H. A. Haus, J. Foresi, and J.-P. Lain, J. Lightwave Technol. **15**, 1149 (1997).
[13] J. D. Joannopoulos, R. D. Meade, and J. N. Winn, *Photonic Crystals* (Princeton University Press, Princeton, 1995).
[14] P. R. Villeneuve, S. Fan, and J. D. Joannopoulos, Phys. Rev. B **54**, 7837 (1996).
[15] For a review, see K. S. Kunz and R. J. Luebbers, *The Finite-Difference Time-Domain Methods* (CRC Press, Boca Raton, FL, 1993).
[16] J. C. Chen and K. Li, Microwave Opt. Technol. Lett. **10**, 319 (1995).